Carbon Foam Derived from Co-carbonization of Lignin and Petroleum Asphalt for High-efficiency Solar Evaporators

Jiawei Shang[a], Wangda Qu[b], Chen Liang[a], Linghong Yin[b], Ming Li[a]*, Jing Liu[c]

[a.] College of Chemistry and Pharmacy, Qingdao Agricultural University, Qingdao, 266109, China

[b.] Laboratory of Lignin-based Materials, College of Life Sciences, Qingdao Agricultural University, Qingdao, 266109, China

[c.] College of New Materials and New Energies, Shenzhen Technology University, Shenzhen, 518116, China

Supplementary Equations:

The absorption rate (α) of sample was calculated as follows:

$$\alpha = \frac{\int_{200nm}^{2500nm} [1 - R(\lambda)]S(\lambda)d\lambda}{\int_{200nm}^{2500nm} S(\lambda)d\lambda} \tag{1}$$

Where $R(\lambda)$ is the reflectance of the absorber at wavelength λ, and $S(\lambda)$ is the solar spectral irradiance (W m^{-2} nm^{-1}) referred to as solar radiant flux density per unit area.

The evaporation rate of the sample was calculated as follows:

$$v = \frac{\Delta m}{S \cdot t} \tag{2}$$

The solar-to-vapor conversion efficiency (η, %) of the sample was calculated as follows:

$$\eta = \frac{V \cdot h_{LV}}{C_{opt} \cdot q^i} \tag{3}$$

Where Δm, s, t, h_{LV}, C_{opt} and q_i are the water mass reduction during the evaporation time (kg), evaporator area (m^2), evaporation time (h), water evaporation enthalpy (kJ kg^{-1}), the optical concentration and the solar irradiation intensity (1 kW m^{-2}), respectively.

Supplementary Figures:

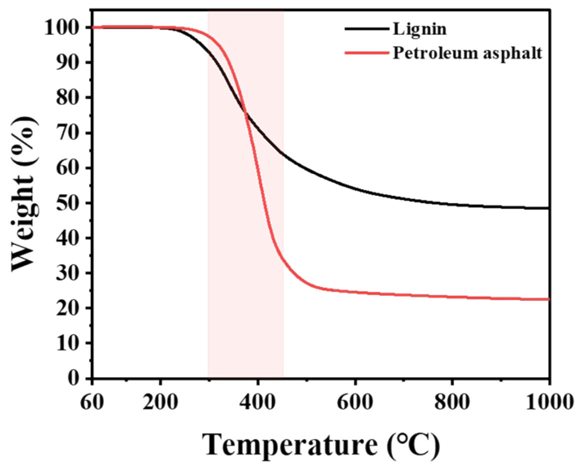

Fig. S1. TG curves of lignin and petroleum asphalt.

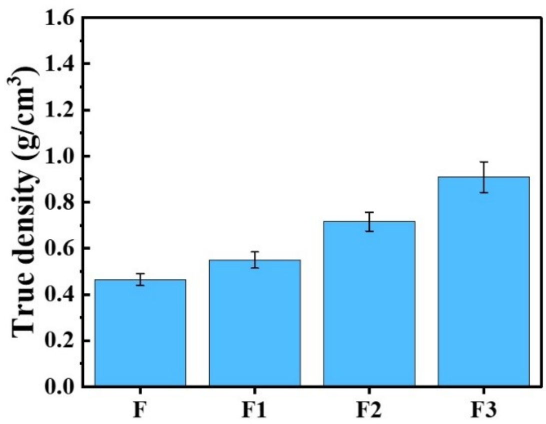

Fig. S2. True densities of F-F3 samples

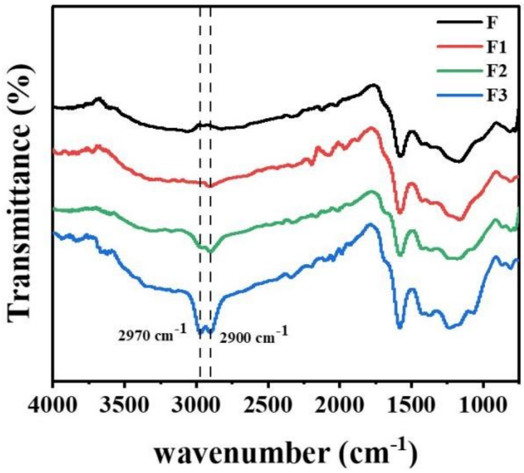

Fig. S3. Infrared spectrogram of F-F3 samples.

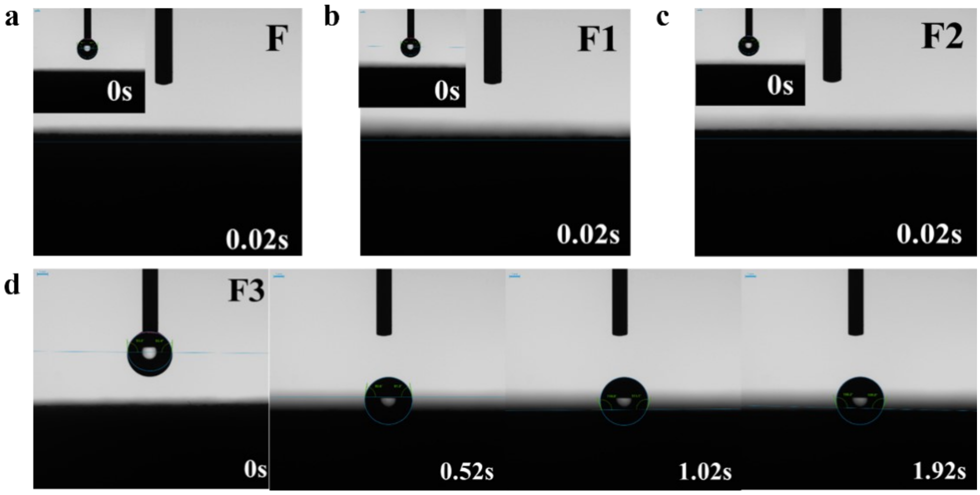

Fig. S4. (a) Contact angle test for F sample; (b) Contact angle test for F1 sample; (c) Contact angle test for F2 sample; (d) Contact angle test for F3 sample.

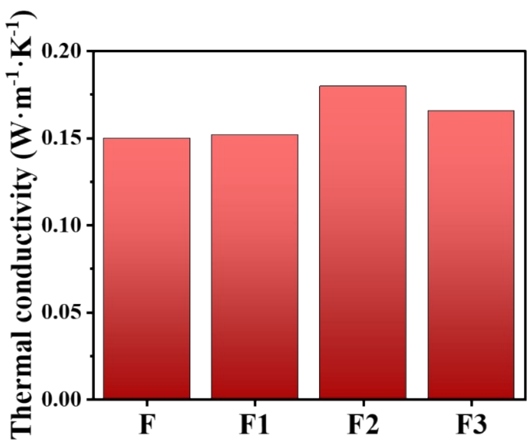

Fig. S5. Thermal conductivity of F-F3 samples.

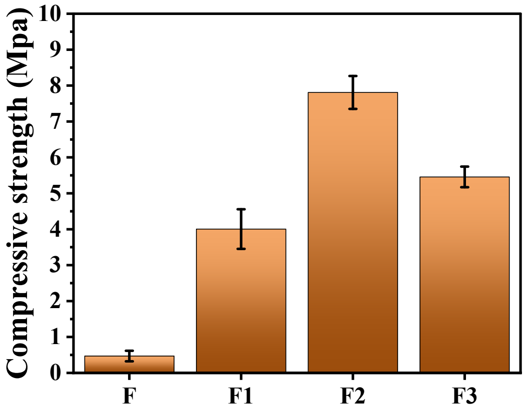

Fig. S6. Compression strength of F-F3 samples.

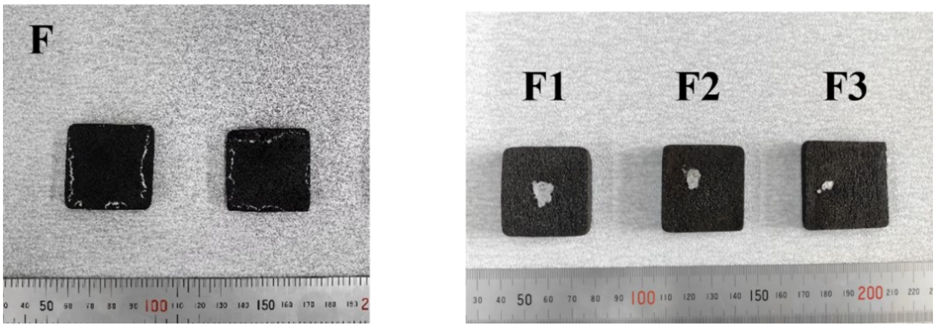

Fig. S7. The phenomenon of salt deposition on the surface of F-F3 samples.

a

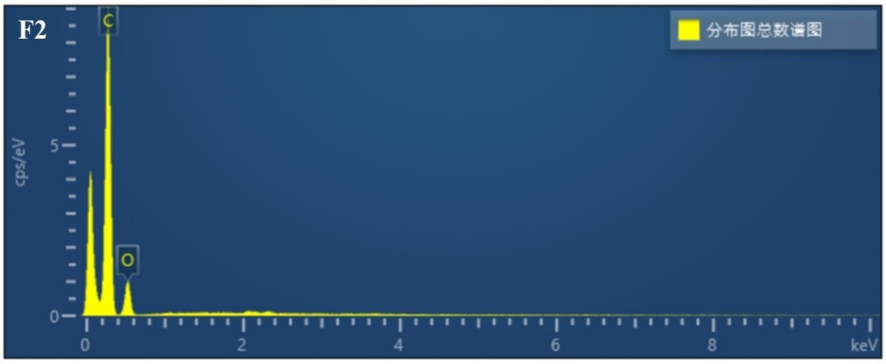

Total number spectrum of distribution map						
Element	Line style	Apparent concentration	K ratio	Wt%	Wt% Sigma	Standard sample label
C	K-line system	135.76	1.35762	78.30	0.40	C Vit
O	K-line system	22.35	0.07523	21.70	0.40	SiO2
Total amount				100.00		

b

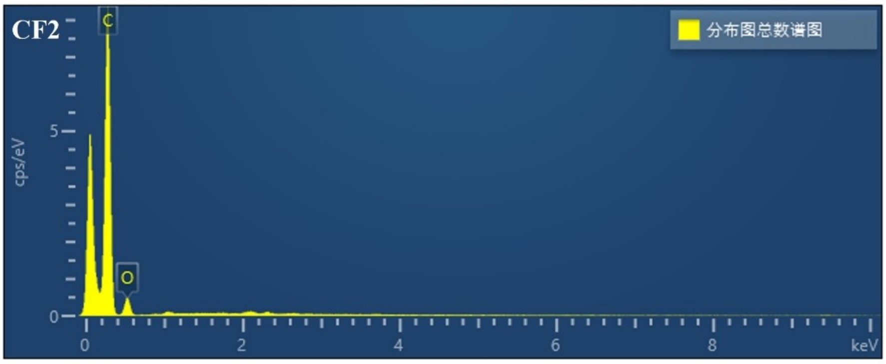

Total number spectrum of distribution map						
Element	Line style	Apparent concentration	K ratio	Wt%	Wt% Sigma	Standard sample label
C	K-line system	129.06	1.29055	85.25	0.34	C Vit
O	K-line system	11.00	0.03703	14.75	0.34	SiO2
Total amount				100.00		

Fig. S8. EDS maps of F2 and CF2 samples

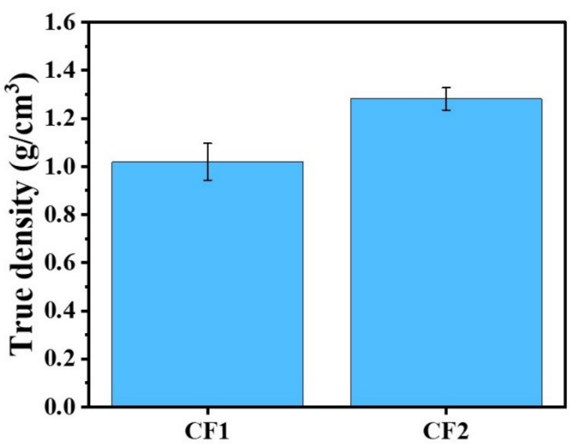

Fig. S9. True densities of CF1, CF2 samples

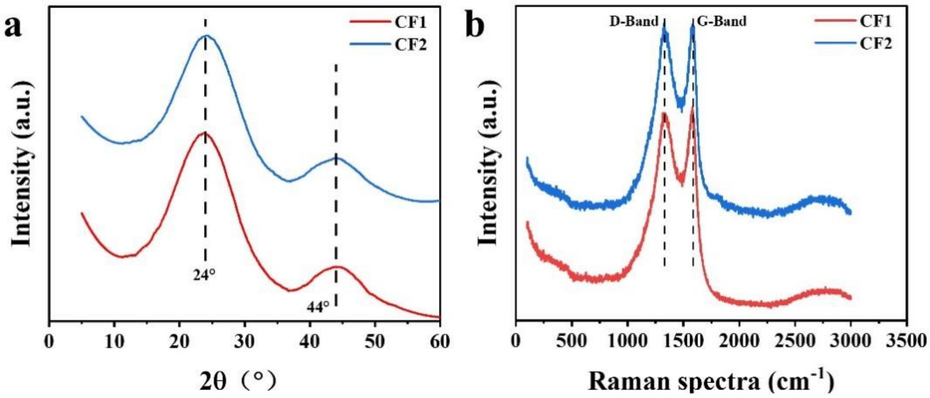

Fig. S10. (a) XRD spectra of CF1 and CF2 samples; (b) Raman spectra of CF and CF2 samples.

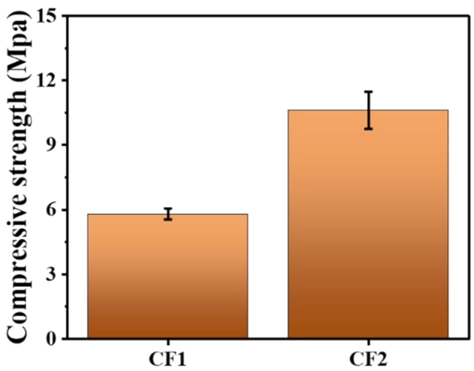

Fig. S11. Compression strength of CF1 and CF2 samples.

Supplementary Figures:

Table S1. Thermal conductivity of different materials for solar steam generation.

No.	Material	Thermal Conductivity ($W\ m^{-1}\ k^{-1}$)	Reference
1	Aerogel-based evaporator	0.066-0.058	1
2	Carbonized corncobs evaporator	0.317	2
3	Carbonized pomelo peel evaporator	0.323	3
4	Lignocellulosic biomass-based evaporator	0.06	4
5	Hydrophilic porous carbon foam evaporator	0.068	5
6	Lignin-based carbon foam (ACF) solar interface evaporator	0.023	6
7	Mesoporous cellulose-based hydrogel	0.719	7
8	Lignin-petroleum asphalt composite carbon foam (CF1, CF2)	0.093-0.1	This study

Table S2. Evaporation rate of water under standard sunlight in interfacial solar seawater desalination with different materials.

No.	Material	Evaporation rate ($kg\ m^{-2}\ h^{-1}$)	Reference
1	sunflower heads solar interface evaporator	1.51	8
2	loofah (CL) solar interface evaporator	1.72	9
3	carbonized banana foam (CBF) solar interface evaporator	1.51	10
4	MOF solar interface evaporator	1.97	11
5	CuS–CF solar interface evaporator	1.90	12
6	bamboo-based solar interface evaporator	1.63	13
7	3D fabric-base solar interface evaporator	1.57	14
8	corn cob-base solar interface evaporator	1.68	15
9	Lignin-based carbon foam (ACF) solar interface evaporator	2.11	6
10	Lignin-petroleum asphalt composite carbon foam (CF2)	2.04	This study

Reference:

1. Sun, M., Ji, X., Li, M., Yu, Y., Zhang, K., Wang, C., and Yang, H. Anisotropic solar evaporator with low thermal conductivity for desalination, thermoelectric generation and cultivation. *Separation and Purification Technology*, 2025, ***369***, 133124.

2. Chen, T. J., Xie, H., Qiao, X., Hao, S. Q., Wu, Z. Z., Sun, D., Liu, Z. Y., Cao, F., Wu, B. H., and Fang, X. L. Highly Anisotropic Corncob as an Efficient Solar Steam-Generation Device with Heat Localization and Rapid Water Transportation. ACS Applied Materials & Interfaces, 2020, **12**, 50397-50405.

3. Liu, X. H., Mishra, D. D., Li, Y. K., Gao, L., Peng, H. Y., Zhang, L., and Hu, C. Q. Biomass-Derived Carbonaceous Materials with Multichannel Waterways for Solar-Driven Clean Water and Thermoelectric Power Generation. ACS Sustainable Chemistry & Engineering, 2021, **9**, 4571-4582.

4. Sun, Y., Zhao, Z. B., Zhao, G. Y., Wang, L. X., Jia, D. Z., Yang, Y. Z., Liu, X. G., Wang, X. Z., and Qiu, J. S. High performance carbonized corncob-based 3D solar vapor steam generator enhanced by environmental energy. Carbon, 2021, **179**, 337-347.

5. Wang, C., J. Wang, J., Li, Z., Xu, K., Lei, T., Wang, W., Superhydrophilic porous carbon foam as a self-desalting monolithic solar steam generation device with high energy efficiency, J. Mater. Chem. A, 2020, **8**, 9528–9535.

6. Liang, C., Xia, H., Yin, L., Du, C., Wu, X., Wang, J., Li, S., Xu, J., Zhang, X., Wang, Y., and Qu, W. Carbon foam directly synthesized from industrial lignin powder

as featured material for high efficiency solar evaporation. Chemical Engineering Journal, 2024, **481**, 148375.

7. Sun, Z., Li, Z., Li, W., and Bian, F. Mesoporous cellulose/TiO2/SiO2/TiN-based nanocomposite hydrogels for efficient solar steam evaporation: low thermal conductivity and high light-heat conversion. *Cellulose*, 2020, **27**, 481-491.

8. Sun, P., Zhang, W., Zada, I., Zhang, Y., Gu, J., Liu, Q., Su, H., Pantelić, D., Jelenković, B., and Zhang, D. 3D-Structured Carbonized Sunflower Heads for Improved Energy Efficiency in Solar Steam Generation. *ACS Applied Materials & Interfaces*, 2020, **12**, 2171-2179.

9. Zhang, C., Yuan, B., Liang, Y., Yang, L., Bai, L., Yang, H., Wei, D., Wang, F., Wang, Q., Wang, W., and Chen, H. Carbon nanofibers enhanced solar steam generation device based on loofah biomass for water purification. *Materials Chemistry and Physics*, 2021, **258**, 123998.

10. Ma, S., Wu, Y., Lv, R., Gao, X., and Wang, Q. Mechanically robust biomass-derived carbonaceous foam for efficient solar water evaporation. *New Journal of Chemistry*, 2022, **46**, 21771-21779.

11. Chen, G., Jiang, Z., Li, A., Chen, X., Ma, Z., and Song, H. Cu-based MOF-derived porous carbon with highly efficient photothermal conversion performance for solar steam evaporation. *Journal of Materials Chemistry A*, 2021, **9**, 16805-16813.

12. Hussain, M., Taranova, A., Ibrahim, K. B., Gradone, A., Rodríguez-Castellón, E., Gross, S., Morandi, V., Moretti, E., Vomiero, A., and Shifa, T. A. Decoration of Two-Dimensional Cus Nanoflakes on Graphitic Carbon Foam Derived from Waste

Plastic for Interfacial Solar Desalination. *Solar RRL*, 2025, **9**, 2400777.

13. Li, J., Yao, H., Su, J., Tan, N., Zhou, T., and Shi, L. A Bionic Ripple Bamboo Based Solar Interface Evaporator for High Efficiency Seawater Desalination. Journal of Bionic Engineering, 2025, **22**, 3095-3107.

14. Zhang, X., Pan, J., Zhu, Y., Hai, W., Zhang, Y., Li, M., Zhang, B., Jiang, J., Bi, S., Shao, H., Chen, N., and Shao, G. Inspired by turtle: 3D raised knitted solar evaporator achieves efficient seawater desalination. Desalination, 2025, **614**, 119191.

15. He, J., Ge, J., Pang, Y., Shen, L., Wu, Y., Lv, Y., Zhang, B., Peng, L., Yang, J., and Qu, M. A 3D Corncob-based interfacial solar evaporator enhanced by environment energy with salt-rejecting and anti-corrosion for seawater distillation. Solar Energy, 2023, **252**, 39-49.